Inhibiting Vimentin or beta1-integrin Reverts Prostate Tumor Cells in lrECM and Reduces Tumor Growth

*Xueping Zhang[1], *Marcia V. Fournier[2], Joy L. Ware[3], Mina J. Bissell[2] and Zendra E. Zehner[1+] [1]Departments of Biochemistry/Molecular Biology and [3]Pathology, and The [1,3]Massey Cancer Center, Virginia Commonwealth University, School of Medicine, Richmond VA 23298-0614, [2]Life Sciences Division, Lawrence Berkeley National Laboratory, Berkeley, CA 94720

+Corresponding Author: Zendra E. Zehner, Ph.D.

P.O. Box 980614

Department of Biochemistry

Virginia Commonwealth University

Richmond, VA 23298-0614

Phone: 804-828-8753

Fax: 804-828-1473

E-mail: zezehner@vcu.edu

*X. Z. and M.V.F. contributed equally to this work.

Keywords: prostate, 3D culture, tumor progression, vimentin, β1-integrin, microenvironment

Abstract

Prostate epithelial cells grown embedded in laminin-rich extracellular matrix (lrECM) undergo morphological changes that closely resemble their architecture *in vivo*. In this study, growth characteristics of three human prostate epithelial sublines derived from the same cellular lineage, but displaying different tumorigenic and metastatic properties *in vivo,* were assessed in three-dimensional (3D) lrECM gels. M12, a highly tumorigenic and metastatic subline, was derived from the parental prostate epithelial P69 cell line by selection in nude mice and found to contain a deletion of 19p-q13.1. The stable re-introduction of an intact human chromosome 19 into M12 resulted in a poorly tumorigenic subline, designated F6. When embedded in lrECM gels, the non-tumorigenic P69 line produced acini with clearly defined lumena. Immunostaining with antibodies to β-catenin, E-cadherin or α6-, β4- and β1-integrins showed polarization typical of glandular epithelium. In contrast, the metastatic M12 subline produced highly disorganized cells with no evidence of polarization. The F6 subline reverted to acini-like structures exhibiting basal polarity marked with integrins. Reducing either vimentin levels via siRNA interference or β1-integrin expression by the addition of the blocking antibody, AIIB2, reorganized the M12 subline into forming polarized acini. The loss of vimentin significantly reduced M12-Vim tumor growth when assessed by subcutaneous injection in athymic mice. Thus, tumorigenicity *in vivo* correlated with disorganized growth in 3D lrECM gels. These studies suggest that the levels of vimentin and β1-integrin play a key role in the homeostasis of the normal acini in prostate and that their dysregulation may lead to tumorigenesis.

Introduction

The extracellular environment is essential for establishing and maintaining cell differentiation during glandular morphogenesis (1). In the developing prostate, budding urogenital epithelial cells attach to the extracellular matrix (ECM) through integrin receptors and migrate into the mesenchyme to form acini containing lumena with established cell polarity (2,3). Integrins play an important role in the bi-directional communication between the cell and the ECM, a process essential for the maintenance of tissue morphology and cellular function. Seminal studies using mammary epithelial cells have shown that the balance of integrin levels is a key regulator of cellular behavior (4). Breast tumor cells, which presented an unbalanced ratio of β1- and β4-integrins, could be restored to a normal cellular phenotype displaying acinar polarity by restoring normal integrin ratios with a blocking β1-integrin antibody (5). Furthermore, integrin signaling has been implicated in tumor–related signaling through FAK, SRC activation correlating with tumor progression and metastasis (6). In prostate cancer, tumor stromal interactions have been found to influence cancer progression (7). Abnormal stroma containing cancer-associated fibroblasts promoted carcinogenesis of non-tumorigenic, genetically abnormal epithelial cells, but had no effect on normal epithelial cells. Growth of cells in three-dimensional (3D) environments, which better mimic the normal cellular microenvironment, offer unique approaches for elucidating signals that contribute to tumor progression *in vivo* (8).

The expression patterns of integrins are known to change during prostate tumor progression. The β1-integrin levels increase in prostate tumor samples, particularly at the cell surface, whereas β2 and β3 remain unchanged (9). Not only do α-integrins change from α6 to α3 in malignant tumor samples, but a shift in binding partner was detected by the retention of the known laminin-1 receptor, α6β1 and a loss of α6β4 (10). Since α6β1 integrin is the leading candidate for conferring invasive potential, it was proposed that inhibition of either α6 or β1 might reverse the invasive phenotype (11). Furthermore, αvβ3 integrin was shown to be important for the progression of prostate cancer to bone and in IGF-regulated signaling (12,13).

Prostate tumors also display a loss of E-cadherin and a switch from intermediate filament proteins (IFP) to vimentin, resulting in loss of hemidesmosomes (11). E-cadherin and vimentin are known markers for epithelial versus mesenchymal cells, respectively. This switch in expression may reflect cells that have undergone an epithelial to mesenchymal transition (EMT), a process that occurs in reverse (the MET) during embryogenesis, but also during tissue development, e.g., in mammary gland branching (14). In cancer, the EMT may be a step towards tumor invasion, although this hypothesis remains controversial (15-17). However, a role for vimentin in motility has been documented in several cell types and may be important in cancer where motility is one component necessary to establish a metastatic phenotype. Fibroblasts where vimentin expression has been eliminated by gene knockout, fail to move in wound healing studies (18-19). In scratch-wound migration assays as well as collagen gel invasion experiments, migration of both breast (MDA-MB-231) and colon (SW480) cancer cells was markedly affected by a 70% reduction in vimentin induced by siRNA approaches (20). Likewise, reducing vimentin expression in the highly invasive MDA-MB-231 human breast cancer cell line resulted in a dramatic decrease in migratory ability *in vitro* (21). MCF7 breast cancer cell lines which lack vimentin are not invasive. Similar studies in MCF10A cells showed that vimentin is functionally involved in the migratory status of human epithelial cells (22). Although comparable studies are lacking in prostate, the expression of vimentin may be an underappreciated component of prostate tumor growth and progression.

Normal methods for culturing cells on plastic tissue culture dishes, referred to as two dimensional (2D) do not duplicate the natural milieu surrounding epithelial cells *in vivo* nor do they produce polarized acini surrounded by basement membrane, as found in normal prostate tissue (23). To better duplicate growth and differentiation, investigators have begun to culture epithelial cells in 3D laminin-rich ECM gels (lrECM) referred to as Matrigel. Matrigel, prepared from the basement membrane of an EHS (Engelbreth-Holm-Swarm) mouse sarcoma, is highly enriched in laminin plus collagen IV, heparin sulfate proteoglycan, entactin and nidogen (24). Since cells grown in lrECM gels closely duplicate glandular phenotypic characteristics, these cultures enable an

investigation into the influence of ECM and stroma on cell growth and differentiation *in vitro* (24-26).

Such approaches have begun to be applied to a variety of prostate epithelial cell lines grown on top of lrECM gels or on individual ECM components such as laminin or fibronectin alone (27,28). For example, the non-tumorigenic prostate epithelial cell line, RWPE-1 immortalized with HPV18 was plated on top of lrECM gels, and it's ability to migrate into- and form branches terminating in- acini was confirmed in 3D cultures (2). Similar cultures of RWPE-2, a Ki-ras transformed, tumorigenic subline of RWPE-1, resulted in single to small clumps of cells with no evidence of acinus organization whereas the unrelated human prostatic carcinoma cell line DU-145 formed amorphous balls without organization or lumen (2). NMU-transformed RWPE-1 cells (WPE1-NB26) formed solid cell masses lacking α6 and β4 integrins with diffuse expression of β1-integrin (29). On the other hand, normal PNT2-C2 cells grown embedded in lrECM gels formed smooth spheroids of tightly packed cells (28). The PC-3 cell line (derived from a bone metastasis) formed a mix of both smooth and irregular spheroids, which had a lumen surrounded by a single cell layer (30). Thus, considerable variability in the morphological structures formed by these different prostate cell lines has been observed. These results could be due to the comparison of genetically dissimilar cell lines or related sublines, which were plated on top of Matrigel rather than embedded. Due to these inconsistent results, we initiated a more thorough analysis of the morphological structures formed by a unique set of genetically related, malignant or non-malignant prostate sublines grown embedded in lrECM gels.

Prostate epithelial cells were immortalized with SV40 large T-antigen to form a non-metastatic, parental cell line referred to as P69 (31,32). The P69 cell line is AR^-, does not secrete PSA, but does express cytokeratin 5 and therefore, may have originated from a more basal origin rather than a differentiated luminal epithelial cell. P69 cells were injected subcutaneously into athymic nude mice and after three *in vivo* passages, a highly metastatic M12 subline was derived (31). Analysis of M12 chromosomal alterations by GTG-banding and FISH detected a novel 16:19 unbalanced translocation resulting in the deletion of one copy of 19p-q13.1. Microcell-mediated

chromosome transfer restored an intact, neomycin-marked human chromosome 19 (Chr19) to generate the F6 subline (33). The M12 subline is fast growing and highly aggressive whereas the F6 subline is slow growing, barely forms small tumors in athymic nude mice, and is not aggressive. These related sublines present an excellent model for investigating requirements for prostate cancer tumor progression.

Here, the behavior of the cytogenetically related and defined P69, M12 and F6 human prostate epithelial sublines was analyzed in 3D cultures. Under these conditions, we found distinct differences in their morphological properties, which correlated with their behavior *in vivo*. The non-metastatic P69 cell line forms polarized acini whereas the metastatic M12 subline was highly disorganized with no evidence of polarization. However, M12 cells reverted to organized acini with the restoration of a second copy of chromosome 19 in forming the F6 subline. Addition of blocking antibodies to β1-integrin or the stable repression of vimentin expression via siRNA technologies allowed the M12 cells to form organized acini structures.

Materials and Methods

Substrates and antibodies. Commercially prepared reconstituted basement membrane, lrECM referred to as Matrigel, (BD Bioscience, Bedford, MA) was used for 3D cultures. Antibodies used for Western blotting and immunostaining studies were as follows: E-cadherin (BD Bioscience, San Jose, CA), β-catenin (H-102: Santa Cruz Biotech., Santa Cruz, CA), β1-integrin (MAB1951Z: Chemicon, Temecula, CA), α6-integrin (MAB1378: Chemicon), β4-integrin (MAB2058: Chemicon), Ki-67 (clone MIB: Jackson ImmunResearch Labs., West Grove, PA), vimentin (V6630: Sigma, St. Louis, MO) and β–actin (A5441: Sigma, St. Louis, MO). FITC-conjugated anti-rat IgG was from Jackson ImmunoResearch Laboratories whereas fluorescent Alexa488/546-labeled anti-rabbit and mouse IgG were from Invitrogen (Carlsbad, CA). Nonspecific rat and mouse IgG and HRP-conjugated secondary antibodies were from Santa Cruz Biotech. Goat $F(ab')^2$ anti-mouse IgG was from Invitrogen (MAB35000).

Cell culture and stable transfectants. The establishment, maintenance and characterization of the SV40 large T antigen-immortalized human prostate epithelial cell

sublines, P69, M12, and F6 have been previously described (31,33,34). M12 cells were stably transfected with a plasmid psiREN-RetroQ (BD Biosciences, San Jose, CA) expressing a human vimentin siRNA (M12-Vim) of sequence 5'-GATCCG-CACCGAGTTCAAGAACACCTTTTCAAGAGAGGTGTTCTTGAACTCGGTGTTCTTTT-TTTCTAGAG-3' [the human vimentin gene sequence is underlined] kindly provided by Dr. A. Yuedell (Phillips Dental Institute, VCU). M12 cells transfected with either the empty pSiREN-RetroQ vector (M12siREN) or vector containing a non-targeting control sequence (M12-NTC: 5'-GATCCGGCATGTACTAGCCTAAGCGTTTTCAAGAGACGC-TTAGGCTAGTACATGCTTCTTTTTTTCTAGAG-3') served as negative controls. A search of the human genome or Sanger microRNA database confirmed no significant match to the non-targeting control sequence. Cells were transfected using *Trans*IT-LT1 transfection reagent (Mirus Bio Corp., Madison, WI) according to manufacture's instructions. Puromycin-resistant cells were selected in 400 ng/ml puromycin (Amersham Biosciences, Piscataway, NJ) and maintained with 100 ng/ml puromycin. The down-regulation of vimentin gene expression in stable transfectants designated as M12-Vim was confirmed by Western blot analysis.

3D Matrigel cell culture. 3D cultures were prepared by growing prostate cancer cells to 80% confluence of monolayer on plastic tissue culture dishes, followed by trypsinization and collection by centrifugation. Matrigel was pre-thawed on ice overnight. 1×10^6 cells were mixed with 1 ml of Matrigel and added to each well of a 6-well dish. Following 1 hour incubation at 37^{o}C, the Matrigel had polymerized. Medium (1-2 ml) containing a specific drug, if needed as cited above, was added on top of the solidified Matrigel-cell mix (33). The medium was replaced every other day. Cultures were routinely grown for 2-16 days in Matrigel.

***In vivo* tumorigenicity assays.** Tumorigenicity of M12 cells stably transformed with the vimentin siRNA expression plasmid (M12-Vim), vector alone (M12-siREN), or vector expressing the non-targeting RNA control (M12-NTC), was assessed by subcutaneous injection of 1×10^6 cells into athymic nude mice as described previously (31). A total of 15 mice were injected as follows: 6 mice with M12-Vim, 4 mice with M12-siREN and 5 mice with M12-NTC for a total of 9 mice serving as negative controls.

Tumor growth was monitored by caliper measurement for up to 42 days and approximate tumor volume (mm^3) was calculated as length X $width^2/2$. At the time of euthanasia, tumors were removed, samples fixed in 10% buffered formalin, paraffin-embedded, stained, and examined for vimentin expression. All experiments were conducted under a protocol approved by the Institution Animal Care and Use Committee of Virginia Commonwealth University.

Western immunoblotting. Cells were washed with cold 1×PBS and then lysed in 4% SDS in 1×PBS with protease inhibitor cocktail (Sigma, St. Louis, MO). After brief sonication, an equal volume of 1×PBS was added to the lysates to reduce the SDS concentration to 2%. Lysates were then centrifuged for 10 min at high speed, supernatants collected and protein concentration measured using the BioRad D_c Protein Assay kit (BioRad, Hercules, CA). Equivalent amounts of protein (~ 40 μg) were boiled in 1×SDS sample buffer for 5 min and analyzed on 8-16% gradient polyacrylamide gels (NuSep Inc., Austell, GA). Western immunoblot analysis was performed as previously described (35).

Indirect immunofluorescence. A sample (≅10 μl) of Matrigel culture was spread on 4-well chamber slides, air dried and fixed in 1:1 methanol-acetone at −20°C for 10 min. The slides were washed by 1×PBS briefly, followed by 400μl 1×IF buffer (130mM NaCl, 7mM Na_2HPO_4, 3.5mM NaH_2PO_4, 7.7mM NaN_3, 0.1% bovine serum albumin, 0.2% Triton X-100, 0.05% Tween-20) with 10% goat serum and a secondary blocking in 200μl 1×IF buffer with 10% goat serum and 20μg/ml goat anti-mouse $F(ab')_2$ fragment for 1 h sequentially. Slides were incubated with primary antibody overnight at 4°C followed directly by either FITC or Alexa-conjugated secondary antibody (1:200) for 45 min. The dilution of antibodies used were as follows: E-cadherin (1:200), β-catenin (1:100-200), vimentin (1:200), Ki-67 (1:200), α6-integrin (1:100), β1-integrin (1:100), β4-integrin (1:100). Nuclei were counterstained with di-amino-phenyl-indole (DAPI, Sigma, St. Louis, MO) overnight at room temperature. Control slides were stained with secondary antibody only. Slides were visualized under LZM5100 confocal Microscope according to the manufacturer's instructions.

Reversion assay. Equal densities of cells were seeded in Matrigel containing AIIB2 (160 μg/ml), a β1-integrin function-blocking monoclonal antibody, or DMSO as control. After 10 days, cells were photographed and stained with specific antibodies as discussed above.

Results

Morphological properties of P69, M12 and F6 sublines grown embedded in lrECM gels. When grown on plastic tissue culture dishes (2D), the cellular morphology of these prostate cell sublines is indistinguishable (Fig. 1*A*, top row). However, when grown embedded in lrECM gels in 3D, these genetically similar sublines organize into distinct, different morphological structures (Fig. 1*A*, bottom row). The non-tumorigenic P69 epithelial cell line organizes into multicellular spheroids referred to as acini (lane 1). Although the highly metastatic M12 subline appears to initially try to form acini, within 24 hrs the cells migrate out of these structures and quickly penetrate and spread throughout the Matrigel (lane 2). The poorly tumorigenic F6 subline (M12s with a restored Chr 19) reverts back to forming acini (lane 3). These morphological differences are retained for at least 20 days when cultured in lrECM gels (see Fig. 3). Moreover, these morphological differences correlate with the differential behavior of these cells upon subcutaneous or orthotopic injection into male, athymic nude mice (33). The M12 subline is highly aggressive and metastasizes to lymph nodes, lung and other organs whereas the F6 subline is poorly tumorigenic and does not metastasize.

A proteomic analysis of these sublines revealed a notable difference in the expression of the IFP, vimentin (34). Epithelial cells grown on plastic tissue culture dishes often aberrantly express vimentin (Fig. 1*B*, top row) albeit at a low level compared to the cytokeratins, the IFPs normally expressed in epithelial cells *in vivo* (36). When grown in 3D, vimentin is not expressed in the P69 subline, akin to expression patterns *in vivo* (Fig. 1*B*, bottom row). Similar to most, if not all metastatic cancers, vimentin is highly expressed in the metastatic M12 subline grown either in 2D or 3D (37). On the other hand, the amount of vimentin protein is severely reduced in the F6 subline grown under either condition (34). Thus, in both cases the M12 subline

highly expresses vimentin, while the P69 and F6 sublines either do not or exhibit a marked decrease in vimentin expression when grown in lrECM gels.

Blocking vimentin via siRNA interference causes dramatic change in the *in vitro* phenotype of M12 cells. Previous studies of non-isogenic breast cancer cell lines suggested that vimentin expression is essential, but not sufficient to cause tumor metastasis (38,39). In our prostate sublines there is a tremendous difference in the amount of vimentin between the metastatic M12 versus its non-metastatic F6 subline (34). To determine if vimentin content could have a direct effect on the morphology of the M12 subline, M12s were stably transformed with a vimentin siRNA producing plasmid and designated M12-Vim. When grown as either 2D or 3D the level of vimentin protein was repressed 85% compared to the wild-type M12 (Fig. 1*B*). When grown on 2D, there was no apparent difference between the morphology of the M12 versus M12-Vim sublines (Fig. 1*A*, top row). However, when grown in 3D the M12-Vim subline reverted to smooth, regular acini-like structures (Fig. 1*A*, bottom row).

Phenotypic characteristics of P69 acini recapitulate glandular prostate tissue. The parental epithelial subline P69 forms smooth, regular acini when grown in lrECM gels (Fig. 2*A*). Confocal microscopy of a series of such pictures taken at a fixed plane through an acinus (referred to as a *Z*-stack) and immunostained with α6-integrin confirms the multicellular nature of these acini with a notable, clear lumen. Nuclei are stained blue with DAPI. The similarity of these structures to those formed by prostate glandular epithelium embedded in a matrix of stromal cells is readily apparent (2).

P69, M12, F6 and M12-Vim sublines differ in the expression and localization of vimentin, β-catenin, E-cadherin and various integrins. Protein organization within the morphological structures formed by the various prostate sublines grown in 3D was addressed by immunostaining for vimentin and a variety of relevant membrane and cell-surface proteins (Figs. 2*B*, 2*C* and 2*D*). Nuclei are stained blue with DAPI. Staining for Ki-67 (a proliferation indicator) reveals that nuclei were actively dividing at day 8 (Fig. 2*B*, panels a-d). P69 acini do not express vimentin (Fig. 2*B*, panel a), but do contain β-catenin (a'), E-cadherin (a"), and α6-, α4- and β1-integrins (Figs. 2*C* and 2*D*, panels a

and a') akin to normal prostate epithelial cells. The overlay (Figs. 2*C* and 2*D*, panel a") indicates that both α6β4 and α6β1-integrin are co-localized and polarized on the outside edge of the acini as seen in prostate tissue (10,11,26).

In contrast, the metastatic M12 subline did not form acini at day 8 (Figs. 2*B*, 2*C* and 2*D*, panel b). β-catenin staining of cell:cell junctions confirm that these cellular masses are not organized into acini (Fig. 2*B*, panel b'). In addition, there is a loss of expression of the epithelial cell marker, E-cadherin (panel b"), co-incident with the emergence of vimentin (panel b). A reduction in expression of E-cadherin concomitant with activation of vimentin expression is thought to be indicative of metastatic cells that have progressed through the EMT (15). It would appear that this transition is occurring in these sublines when grown in 3D. Moreover, the M12 cellular mass shows little organization and a loss of polarization as detected by diffuse staining with antibodies to α6-, β1- and β4-integrins (Figs. 2*C* and 2*D*, panels b, b' and b"). Interestingly, the overlay (Fig. 2*C*, panel b") shows some evidence for continued co-localization of α6β4-integrin but less for α6β1-integrin (Fig. 2*D*, panel b") and there is no evidence for polarization in either case. In a time course study, it was evident that at 24 hours the M12 subline did initially try to form acini (a remnant of which is seen in Fig. 2*B*, panel b, white arrow), but by day 8 many cells have migrated out of the acini into the lrECM gel. Staining of these early acini for α6-integrin did hint at some polarization (data not shown), but this polarity was soon lost as cells migrated into the lrECM gel where α6-integrin staining became diffuse.

Restoration of a second copy of Chr19 produced the F6 subline, which is poorly tumorigenic. Interestingly, these F6 cells produce acini-like structures (Figs. 2*B*, 2*C* and 2*D*, panel c). Expression of vimentin is greatly reduced (Fig. 2*B*, panel c) and expression of E-cadherin returns (panel c") with the multicellular nature of these acini confirmed by β-catenin staining of cell junctions (panel c'). Moreover, F6 acini exhibit α6-, β1- or β4-integrin polarization with co-localization of α6β1- and α6β4- integrin dimers (Figs. 2*C* and 2*D*, panels c, c' and c"). The F6 cells are rarely metastatic *in vivo* in male, athymic nude mice and their growth properties in 3D better duplicate normal epithelium (33).

Reducing vimentin expression via siRNA also reverts M12 cells back to acini-like structures (Figs. 2*B*, 2*C* and 2*D*, panel d). Immunostaining with vimentin and E-cadherin antibodies showed that the M12-Vim subline expresses E-cadherin instead of vimentin (Fig. 2*B*, compare panel d" to d). Western blots confirm that P69, F6, or M12-Vim acini grown in lrECM gels (3D) retain E-cadherin expression whereas it is loss in similar cultures of the M12 subline (data not shown). M12-Vim cells exhibit polarization of α6, β1 or β4 integrins and renewed co-localization of $\alpha 6\beta 1$ and $\alpha 6\beta 4$ integrin dimers (Figs. 2*C* and 2*D*, panel d, d' and d"), which is similar to that seen in the P69 or F6 acini (Figs. 2*C* and 2*D*, panels a" and c"). These results imply that vimentin expression plays an important role in attaining the disorganized morphology of the M12 subline grown in lrECM gels.

Measurement of growth rate indicates P69, F6 and M12-Vim growth arrest at day 16. Next, we compared the growth properties of P69, F6 and M12-Vim structures overtime in 3D culture to determine if acini reach a maximum size (cell number), become growth arrested or maintain a lumen (Fig. 3). Counting the number of nuclei in one hundred P69, F6 and M12-Vim acini indicated these cells are still actively dividing by day 13 in culture (Fig. 3*A*). Growth arrest occurs around day 16, as confirmed by negative staining for Ki-67 at day 16 compared to day 13 (data not shown). The size of the acini (um) also reaches a maximal level by day 16, consistent with the cell number count per acini (Fig. 3*B*). This differs from non-malignant human mammary epithelial cells where growth arrest is observed at day 7 in 3D lrECM gels (40). In contrast, M12 sublines still show positive Ki-67 staining up to day 16. These cultures could not be analyzed past 16 days as the ability of the lrECM gel to support growth becomes rate limiting. Since M12 cells form a non-organized cellular mass rather than acini, it was not possible to count the number of nuclei.

Blocking vimentin expression in M12 cells affects tumor formation in athymic nude mice. Previously, the tumorigenicity of the M12 and F6 subline was determined by subcutaneous injection into nude mice (33). All mice (13/13) injected with M12 cells developed tumors after 9-15 days. Mice injected with F6 cells either failed to produce tumors (9/15) or produced only small tumors (6/15) after 120 days. When

grown in 3D, reducing the expression of vimentin reverted the M12 cells back to acini-like structures. Next, we asked if the dramatic morphological difference observed *in vitro* would correlate to tumor growth *in vivo*? To answer this question, tumor formation was assessed by subcutaneous injection into nude mice (Fig. 4) of M12 cells stably transformed with vector only (M12-siREN), vector expressing a non-targeting, scrambled RNA sequence (M12-NTC) or M12-Vim. By 42 days 6/6 mice injected with M12-Vim displayed tumors which were over 8-fold reduced in size compared to the average of the 9 mice injected with either the M12-siREN or M12-NTC negative controls. ANOVA test gave p-values <0.01. Importantly, there was little difference in the proliferation rate of the M12-Vim subline compared to the negative control cells in 2D culture (data not shown). Thus, the lack of vimentin is not influencing cell growth rate *in vitro*. At the completion of the experiment, animals were euthanized, tumors were removed, and continued vimentin expression in the M12-siREN negative control verified by immunohistochemical staining (Fig. 4B, left panel). Little vimentin could be detected in the small tumors formed by the M12-Vim subline (Fig. 4B, right panel) in agreement with the original Western blots (Fig. 1).

These *in vitro* and *in vivo* results are compiled in Table 1. A comparison of acini formation versus disorganized growth, accompanied by the expression, localization, co-localization and polarization of relevant proteins, is consistent to that displayed by glandular epithelium in prostate tissue. The tumorigenicity of the original M12 and F6 sublines was documented previously (33). Here, the reduction of vimentin expression in the M12-Vim cells reduced tumor growth compared to the M12 control cells. Overall, these comparisons support the conclusion that the growth of these uniquely related prostate sublines in 3D culture parallels their properties *in vivo* and those of glandular epithelium as cells progress to tumor formation and ultimately metastatic prostate carcinoma.

Inhibiting β1-integrin activity can cause a phenotypic reversion. The inclusion of blocking antibodies for β1-integrin (AIIB2) reverts the M12 cells back to smooth acini-like structures (Fig. 5*A*). Similar treatment of the F6 subline shows little effect, although there may be a slight reduction in acini size. Western blots

demonstrated that AIIB2 treatment did dramatically decrease β1-integrin expression in both the M12 and F6 sublines, whereas vimentin expression in the M12 subline or actin levels in either subline was not affected by AIIB2 treatment (Fig. 5*B*). Immunostaining with the E-cadherin antibody showed that AIIB2 treatment increased E-cadherin expression, resulting in some evidence of polarization akin to F6 acini structures (Fig. 5*C*, panel b' compared to panels c' and d'). Importantly, AIIB2 had little effect on F6 acini formation. Thus, this affect appears to be specific to the M12 cells. This differs from other studies, where acinar formation of normal prostate epithelium was practically obliterated by the addition of either α6- or β1-blocking antibodies (29), but does agree with the fact that β1-integrin is more associated with the formation of focal adhesion complexes involved with motility than stable hemidesmosomal attachment sites used more for the anchoring of cells. To our knowledge, this is the first time that the effect of β1-integrin function-blocking antibodies has been tested against metastatic prostate cells rather than normal prostate epithelial, a more relevant assay for determining how changes in protein expression contribute to tumor progression.

Discussion

The analysis of multiple membrane and cell surface proteins (E-cadherin, β-catenin, and α6-, β1-, β4-integrins) in these 4 genetically related human prostate epithelial cell lines grown in 3D culture demonstrates that the relative distribution and proportion of cell surface integrins controls the structural homeostasis of these cells. Moreover, the *in vitro* expression and distribution of these proteins is functionally related to their behavior *in vivo*. Thus α6-, β1- and β4 integrin expression is polarized in the non-tumorigenic P69 acini, poorly tumorigenic F6 and M12-Vim acini, but disappears in the disorganized mass of highly tumorigenic and metastatic M12 cells.

The growth of the non-tumorigenic parental P69 cell line in 3D culture produces structures that are morphologically similar to human glandular prostate epithelial cells (2). With respect to integrins, these acini are polarized and appropriate integrin pairs are co-localized. The metastatic M12 subline escapes from acini formation and quickly spreads throughout the lrECM gel whereas the non-metastatic, barely tumorigenic F6

subline reverts to the production of more normal, polarized acini-like structures. Thus, a thorough analysis of these genetically related sublines has revealed *in vitro* morphological properties, which correlate with their tumorigenic/metastatic behavior *in vivo* (31-33). These results agree with those previous studies where an inverse relationship was found between acinar formation and malignancy (2,41).

Previously, we found that the expression of vimentin was one of the major differences between the M12 and F6 sublines (34). Recently, a correlation between vimentin expression and degree of metastasis was confirmed in another set of genetically related prostate cells lines (42). This switch in protein expression suggested that these sublines might be undergoing an EMT transition *in vitro*, as the gain of vimentin expression with the concomitant loss of E-cadherin has often been used as a biomarker for EMT (15). More importantly, we found vimentin expression to be a crucial component of this morphological change. Disorganized M12 cells containing vimentin did not form acini in lrECM gels. Rather, these cells rapidly moved out of the acinus after only a few days in culture and by day 9 have spread throughout the lrECM gel with little evidence of any acini structure. M12 cells are both vimentin and Ki-67 positive. On the other hand, P69 and F6 sublines express little vimentin, but did form acini-like structure in lrECM gels. Blocking vimentin gene expression via siRNA reverted M12 cells to producing acini-like structures. These results imply that the lack of vimentin protein is essential for formation of acini-like structures *in vitro*. Furthermore, M12-Vim cells displayed a considerable reduction in tumor growth *in vivo*, consistent with those morphological differences displayed *in vitro*. Although several studies document a requirement for vimentin in motility and invasion assays *in vitro*, this is the first indication of such a dramatic effect on tumor growth *in vivo* dependent upon the continued expression of vimentin (18-22). An increase in β1-integrin expression has been found in actual prostate tumor samples as well as in more de-differentiated tumor cells (9,10). Similar results have been reported for metastatic mammary gland epithelial cell lines, where reversion by the inhibitory β1-integrin antibody or its $F(ab')^2$ fragment led to the re-establishment of E-cadherin-β-catenin complexes (5). Here, the interruption of β1-integrin expression did reverse the morphological phenotype of the metastatic M12 subline back to organized, polarized acini as proposed, but never proven experimentally

(11). In our study we detected an actual increase in expression of E-cadherin in the F6 subline compared to M12s or in M12s reverted by the addition of β1-integrin blocking antibodies. Previously, it was suggested that β1-integrin blocking antibodies could represent a relevant therapy to combat tumor progression in metastatic breast cancer (43). Our results support a similar application to prostate cancer.

Recently, it was postulated that in motile cells vimentin is responsible for moving endocytosed β1-integrin from the rear of the cell to the leading edge under the control of PKC-ε (44). Upon inhibition of PKC-ε and loss of vimentin phosphorylation, integrins become trapped in endocytic vesicles and directional motility towards the ECM is severely attenuated. Other studies have proposed that vimentin functions as a carrier to move cargo on microtubules using kinesin/dynein motors (45,46). Vesicle movement on the IFP network itself has never been documented. Inhibitors that collapse microtubules (MT) also affect the IFP network, suggesting there is cross-talk between MTs and IFs. Since the IFP network is the only cytoskeletal filament that completely traverses the cytoplasm from the plasma to the nuclear membrane, a role in signal transduction has been proposed (47). Until now the nature of the cargo carried by vimentin in non-neuronal cells was unknown.

Based on our results and the literature, we propose that vimentin may contribute to moving β1-integrin to the leading edge to support motility in prostate carcinoma (44). A direct correlation between vimentin and motility has been suggested in several cell types and in cancer as noted earlier (18,19,21,22). Blocking β1-integrin antibodies preferentially affected the cellular behavior of metastatic mammary gland cells in 3D culture and *in vivo,* when injected either subcutaneous or into the fat pad of the mammary gland, whereas non-malignant or normal tissues were not affected (43). Prostate carcinoma are positive for α6β1 expression and expression of α6-integrin, β1-integrin's preferred partner, correlates with a more invasive metastatic phenotype (10,11,48,49). Thus, we propose that vimentin:β1-interaction is crucial for motility, an important precondition for the metastatic property of M12 cells *in vivo*. Blocking this movement by either blocking β1-integrin via specific antibodies or reducing the amount of vimentin protein via siRNA interference reverts cells to acini-like structures. More

importantly, the growth of reverted M12 cells is severely reduced upon subcutaneous injection into nude mice, whereas tumor formation of M12 cells with vector alone or vector expressing a non-targeting siRNA is unaffected. This hypothesis is further supported by the fact it is only the metastatic M12 subline, which expresses both vimentin and β1-integrin, that is highly motile, a required feature for establishing metastasis. We propose that by understanding the nature of the vimentin:β1-integrin interaction, target molecule(s) could be generated to block this interaction. These would be specific for the metastatic cell, since it is only the metastatic cell that expresses both β1-integrin and vimentin. Moreover, this may also produce a relevant target for a variety of other metastatic tumor cells like breast, which also co-express β1-integrin and vimentin at high levels.

In summary, these studies support the concept that the relative distribution and proportion of cell surface integrins serves to maintain the structural homeostasis of prostate epithelial tissues. Growth in 3D presents a biologically relevant model system for further studies into what controls these morphological differences *in vitro,* which could contribute relevant information to what promotes tumor progression *in vivo*. Alterations in the level and distribution of integrins, as well as the cytoskeletal protein vimentin, can lead to aberrant behavior of tumor cells and alter their ability to respond to ECM-generated signals. Growth of these unique prostate sublines in 3D represents a novel approach to detect relevant markers/targets that could be used in the diagnosis, prevention and ultimate treatment of prostate tumor progression. In addition, these sublines and the 3D technology could be easily adapted to high throughput screening for drugs, which could modify M12 morphological behavior *in vitro,* and identify a useful future therapy to counteract high tumor growth rates and/or metastasis *in vivo*.

Acknowledgement

Grant support:

Department of Defense grant DAMD 17-00-1-0296 and Virginia Commonwealth Health Research Board 40-06 (Z.E. Zehner) and U.S. DOE, OBER Office of Biological and Environmental Research, DE-AC0205CH1123, 03-76SF00098 and a Distinguished Fellow Award; NCI awards R01CA064786, R01CA057621,U54CA126552 and U54CA112970; U.S. DOD W81XWH0810736 and W81XWH0510338 (M.J. Bissell).

References

1. Barcellos-Hoff MH, Aggeler J, Ram TG, Bissell MJ. Functional differentiation and alveolar morphogenesis of primary mammary cultures on reconstituted basement membrane. Development 1989;105:223-35.

2. Webber MM, Bello D, Kleinman HK, Hoffman MP. Acinar differentiation by non-malignant immortalized human prostatic epithelial cells and its loss by malignant cells. Carcinogenesis 1997;18:1225-31.

3. Hynes RO. A reevaluation of integrins as regulators of angiogenesis. Nat Med 2002;8:918-21.

4. Streuli CH, Bailey N, Bissell MJ. Control of mammary epithelial differentiation: basement membrane induces tissue-specific gene expression in the absence of cell-cell interaction and morphological polarity. J Cell Biol 1991;115:1383-95.

5. Weaver VM, Petersen OW, Wang F, et al. Reversion of the malignant phenotype of human breast cells in three-dimensional culture and *in vivo* by integrin blocking antibodies. J Cell Biol 1997;137:231-45.

6. Guo W, Giancotti FG. Integrin signalling during tumour progression. Nat Rev Mol Cell Biol 2004;5:816-26.

7. Cunha GR, Hayward SW, Wang YZ, Ricke WA. Role of the stromal microenvironment in carcinogeneiss of the prostate. Int.J.Cancer 2003;107:1-10.

8. Bissell MJ, Rizki A, Mian IS. Tissue architecture: the ultimate regulator of breast. Curr Opin Cell Biol 2003;15:753-62.

9. Murant SJ, Handley J, Stower M, Reid N, Cussenot O, Maitland NJ. Co-ordinated changes in expression of cell adhesion molecules in prostate cancer. Eur J Cancer 1997;33:263-71.

10. Nagle RB, Hao J, Knox JD, Dalkin BL, Clark V, Cress AE. Expression of hemidesmosomal and extracellular matrix proteins by normal and malignant human prostate tissue. Am J Pathol 1995;146:1498-507.

11. Cress AE, Rabinovitz I, Zhu W, Nagle RB. The alpha 6 beta 1 and alpha 6 beta 4 integrins in human prostate cancer progression. Cancer Metastasis Rev 1995; 14:219-28.

12. Marelli MM, Moretti RM, Procacci P, Motta M, Limonta P. Insulin-like growth factor-I promotes migration in human androgen-independent prostate cancer cells via the alphavbeta3 integrin and PI3-K/Akt signaling. Int J Oncol 2006;28:723-30.

13. Cooper CR, Chay CH, Pienta KJ. The role of alpha(v)beta (3) in prostate cancer progression. Neoplasia 2002;4:191-4.

14. Nelson CM, Vanduijn MM, Inman JL, Fletcher DA, Bissell MJ. Tissue geometry determines sites of mammary branching morphogenesis in organotypic cultures. Science 2006;314:298-300.

15. Gilles C, Thompson EW. The epithelial to mesenchymal transition and metastatic progression in carcinoma. The Breast J. 1996;2:83-96.

16. Thompson EW, Newgreen DF, Tarin D. Carcinoma invasion and metastasis: A role for epithelial-mesenchymal transition? Cancer Res 2005;65:5991-5.

17. Tarin D, Thompson EW, Newgreen DF. The fallacy of epithelial mesenchymal transition in neoplasia. Cancer Res 2005;65:5996-6001.

18. Eckes B, Colucci-Guyon E, Smola H, et al. Impaired wound healing in embryonic and adult mice lacking vimentin. J Cell Sci 2000;113:2455-62.

19. Eckes B, Dogic D, Colucci-Guyon E, et al. Impaired mechanical stability, migration and contractile capacity in vimentin-deficient fibroblasts. J.Cell Sci. 1998;111:1897-907.

20. McInroy L, Maatta A. Down-regulation of vimentin expression inhibits carcinoma cell migration and adhesion. Biochem Biophys Res Commun 2007;360:109-14.

21. Hendrix MJ, Seftor EA, Chu YW, Trevor KT, Seftor RE. Role of intermediate filaments in migration, invasion and metastasis. Cancer and Metastasis Rev 1996;15:507-25.

22. Gilles C, Polette M, Zahm JM, et al. Vimentin contributes to human mammary epithelial cell migration. J Cell Sci 1999;112:4615-25.

23. Schmeichel KL, Bissell MJ. Modeling tissue-specific signaling and organ function in three dimensions. J Cell Sci 2003;116:2377-88.

24. Kleinman HK, McGarvey ML, Hassell JR, et al. Basement membrane complexes with biological activity. Biochemistry 1986;25:312-8.

25. Streuli CH, Bissell MJ. Expression of extracellular matrix components is regulated by substratum. J Cell Biol 1990;110:1405-15.

26. Knox JD, Cress AE, Clark V, et al. Differential expression of extracellular matrix molecules and the alpha 6-integrins in the normal and neoplastic prostate. Am J Pathol 1994;145:167-74.

27. Bello D, Webber MM, Kleinman HK, Wartinger DD, Rhim JS. Androgen responsive adult human prostatic epithelial cell lines immortalized by human papillomavirus 18. Carcinogenesis 1997;18:1215-23.

28. Lang SH, Sharrard RM, Stark M, Villette JM, Maitland NJ. Prostate epithelial cell lines form spheroids with evidence of glandular differentiation in three-dimensional Matrigel cultures. Br J Cancer 2001;85:590-9.

29. Bello-DeOcampo D, Kleinman HK, Deocampo ND, Webber MM. Laminin-1 and alpha6 beta1 integrin regulate acinar morphogenesis of normal and malignant human prostate epithelial cells. Prostate 2001;46:142-53.

30. Kaighn ME, Narayan KS, Ohnuki Y, Lechner JF, Jones LW. Establishment and characterization of a human prostatic carcinoma cell line (PC-3). Invest Urol 1979;17:16-23.

31. Bae VL, Jackson-Cook CK, Maygarden SJ, Plymate SR , Chen J, Ware JL. Metastatic sublines of an SV40 large T antigen immortalized human prostate epithelial cell line. Prostate 1998;34:275-82.

32. Bae VL, Jackson-Cook CK, Brothman AR, Maygarden SJ, Ware JL. Tumorigenicity of SV40 T antigen immortalized human prostate epithelial cells: association with decreased epidermal growth factor receptor (EGFR) expression. Int J Cancer 1994;58:721-9.

33. Astbury C, Jackson-Cook CK, Culp SH, Paisley TE, Ware JL. Suppression of tumorigenicity in the human prostate cancer cell line M12 via microcell-mediated restoration of chromosome 19. Genes Chromosomes Cancer 2001;31:143-55.

34. Liu X, Wu Y, Zehner ZE, Jackson-Cook C, Ware JL. Proteomic analysis of the tumorigenic human prostate cell line M12 after microcell-mediated transfer of chromosome 19 demonstrates reduction of vimentin. Electrophoresis 2003;24:3445-53.

35. Zhang X, Diab IH, Zehner ZE. ZBP-89 represses vimentin gene transcription by interacting with the transcriptional activator, Sp1. Nucl Acids Res 2003;31:2900-14.

36. Herrmann ME, Trevor KT. Epithelial-mesenchymal transitions during cell culture of primary thyroid tumors? Genes Chromosomes Cancer 1993;6:239-42.

37. Thompson EW, Paik S, Brunner N, et al. Association of increased basement membrane invasiveness with absence of estrogen receptor and expression of vimentin in human breast cancer cell lines. J Cell Physiol 1992;150:534-44.

38. Hendrix MJ, Seftor EA, Seftor RE, Trevor KT. Experimental co-expression of vimentin and keratin intermediate filaments in human breast cancer cells results in phenotypic interconversion and increased invasive behavior. Am J Pathol 1997;150:483-95.

39. Sommers CL, Heckford SE, Skerker JM, et al. Loss of epithelial markers and acquisition of vimentin expression in adriamycin- and vinblastine-resistant human breast cancer cell lines. Cancer Res 1992;52:5190-7.

40. Fournier MV, Martin KJ, Kenny PA, et al. Gene expression signature in organized and growth-arrested mammary acini predicts good outcome in breast cancer. Cancer Res 2006;66:7095-102.

41. Bello-DeOcampo D, Kleinman HK, Webber MM. The role of alpha 6 beta 1 integrin and EGF in normal and malignant acinar morphogenesis of human prostatic epithelial cells. Mutat Res 2001;480-481:209-17.

42. Wu M, Bai X, Xu G, et al. Proteome analysis of human androgen-independent prostate cancer cell lines: variable metastatic potentials correlated with vimentin expression. Proteomics 2007;7:1973-83.

43. Park C, Zhang H, Pallavicini M, et al. β1 integrin inhibitory antibody induces apoptosis of breast cancer cells, inhibits growth, and distinguishes malignant from normal phenotype in 3D cultures and *in vivo*. Cancer Res 2006;66:1526-35.

44. Ivaska J, Vuoriluoto K, Huovinen T, Izawa I, Inagaki M, Parker PJ. PKCepsilon-mediated phosphorylation of vimentin controls integrin recycling and motility. EMBO J 2005;24:3834-45.

45. Chang L, Goldman RD. Intermediate filaments mediate cytoskeletal crosstalk. Nat Rev Mole Cell Biol 2004;5:601-13.

46. Helfand BT, Chang L, Goldman RD. Intermediate filaments are dynamic and motile elements of cellular architecture. J Cell Sci 2004;117:133-41.

47. Helfand BT, Chou YH, Shumaker DK, Goldman RD. Intermediate filament proteins participate in signal transduction. Trends Cell Biol 2005;15:568-70.

48. Rabinovitz I, Nagle RB, Cress AE. Integrin alpha 6 expression in human prostate carcinoma cells is associated with a migratory and invasive phenotype in vitro and in vivo. Clin Exp Metastasis 1995;13:481-91.

49. Edlund M, Miyamoto T, Sikes RA, et al. Integrin expression and usage by prostate cancer cell lines on laminin substrata. Cell Growth Differ 2001;12:99-107.

Figure legends

Figure 1. Comparison of the morphology of P69, M12, F6 and M12-Vim prostate sublines grown on tissue culture dishes (2D) versus embedded in lrECM (3D). *A*, Light microscopy images of these various prostate cancer sublines were taken from cultures grown in 2D on traditional plastic dishes for 4 days versus 8 days embedded in Matrigel (3D) as described in Materials and Methods. Magnification is at 10X. *B*, Whole cell extracts (40 μg) from 2D and 3D cultures of these sublines were subjected to Western blot analysis with vimentin antibody as described in Materials and Methods. β-actin was used as loading control.

Figure 2: Comparison of content and localization of relevant proteins within the various morphological structures formed by the P69, M12, F6 and M12-Vim prostate sublines grown embedded in lrECM. *A*, A Z-stack of P69 acini from day 8 3D cultures was examined by immunofluorescence confocal microscopy. These 8 pictures represent plane 4, 8, 12, 16, 20, 24, 28 and 32 from 40 such planes. Acini were fixed and stained with antibody to α6-integrin (green) and nuclei counterstained with 4'6-diamidino-2-phenylindole (DAPI; blue) as discussed in Materials and Methods. All pictures are taken at a magnification of 63X. *B*, Confocal immunofluorescence microscopy of structures formed by the various sublines after 8 to 13 days in Matrigel were stained with antibodies to vimentin (green) and Ki-67 (red), panels a thru d; β-catenin (red), panels a' thru d'; and E-cadherin (green), panels a" thru d". Nuclei are stained with DAPI (blue). *C*, Cellular structures were stained with antibodies to α6-integrin (green), panels a thru d, or β4 integrin (red), panels a' thru d'. The overlay of α6β4 integrin is shown in panels a" thru d". Nuclei are stained with DAPI (blue). *D*. Cellular structures were stained with antibodies to α6-integrin (green), panels a thru d, or β1-integrin (red), panels a' thru d'. The overlay of α6β1-integrin is shown in panels a" thru d". Nuclei are stained with DAPI (blue). For details of immunostaining see Materials and Methods. For panels *B*, *C* and *D* a size marker of 5 μm is shown.

Figure 3. Growth properties of P69, F6, and M12-Vim acini in 3D culture. *A,* Acini were isolated from P69, F6 and M12-Vim cultures grown embedded in lrECM gels for 2, 4, 8, 13 and 16 days. The average cell number per acini cross-section (from at least 100 acini) was counted using confocal microscopy. The standard error of the mean is shown as error bars. *B*. The average size of (μm) of acini (from at least 25 acini) was measured as in panel A. The standard error of the mean is shown as error bars.

Figure 4. Tumorigenic properties of M12-Vim cells are reduced in athymic mice. *A,* Tumor formation following subcutaneous injection of 1 X 10^6 M12-Vim cells (6 mice) was compared to the injection of vector only M12-siREN (4 mice) or M12-NTC, containing a nontargeting RNA control, (5 mice) cells. Tumor growth was monitored by caliber measurement each 4 to 5 days for up to 42 days. All animals displayed tumors albeit of varying size and tumor volume (mm^3), calculated as described in Materials and Methods. The standard error of the mean is shown as error bars. The ANOVA test showed p-values of 0.009 and <0.0001 for M12-NTC or M12-siREN, respectively compared to M12-VIM. *B,* Immunohistochemical staining with human vimentin antibody of paraffin-embedded M12-siREN (left panel) and M12-Vim (right panel) tumors retrieved from nude mice at time of euthanasia (42 days). Magnification is at 400X.

Figure 5. Inclusion of the β1-integrin inhibitory antibody (AIIB2) leads to the formation of reverted acini with the metastatic M12 subline. *A,* Light microscopy images of the M12 and F6 subline grown embedded in Matrigel for 10 days in the absence (upper panel) or presence (lower panel) of the β1-integrin, inhibitory antibody, AIIB2 (160 μg/ml). Magnification is at 20X. *B,* Whole cell extracts (40 μg) from 10 day cultures as described in panel *A* were subjected to Western blot analysis with vimentin, β1-integrin, or β-actin antibody. *C,* Confocal immunofluorescence microscopy of the M12 or F6 subline grown embedded in Matrigel for 10 days in the absence or presence of AIIB2 as indicated. Cells were stained with E-cadherin (green) and β-catenin (red) and nuclei were stained with DAPI (blue). Magnification is at 63X and a size marker of 5 μm is shown.

A.

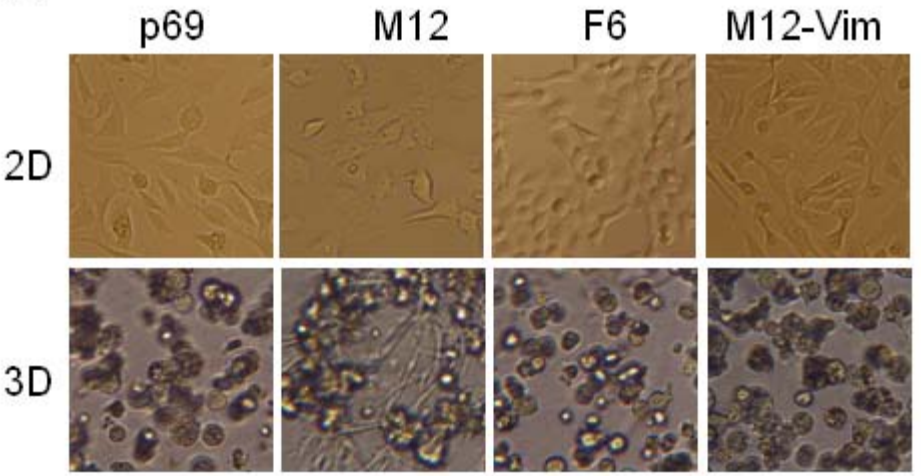
p69
M12
F6
M12-Vim
2D
3D

B.

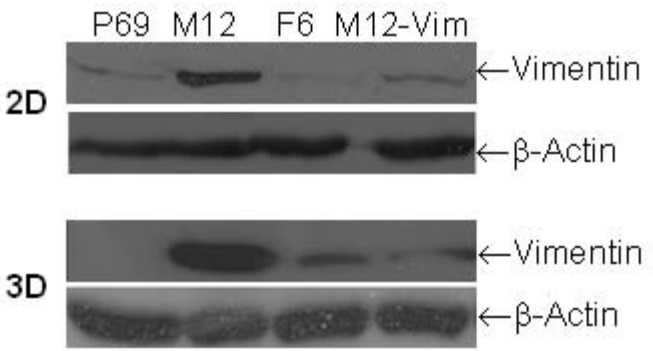
P69 M12 F6 M12-Vim
2D
←Vimentin
←β-Actin
3D
←Vimentin
←β-Actin

Fig. 1

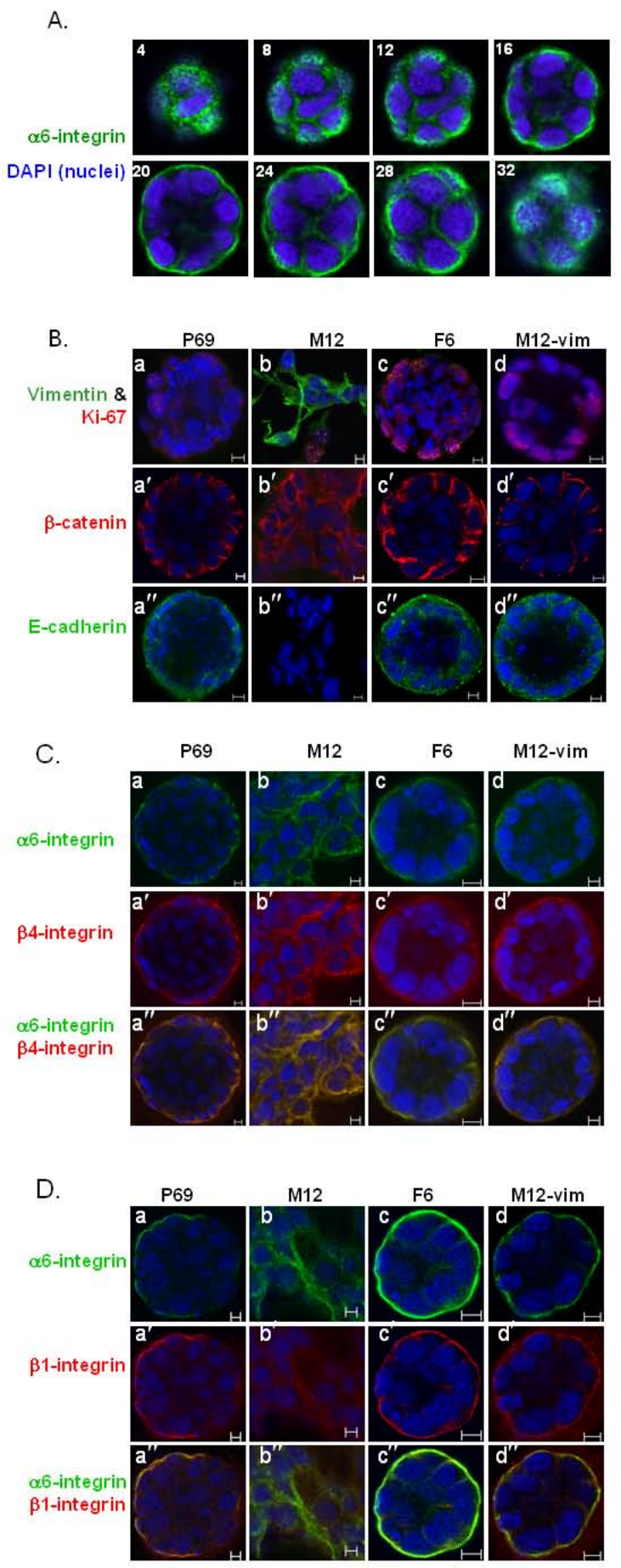
A.
4
8
12
16
α6-integrin
DAPI (nuclei)
20
24
28
32
B.
P69
M12
F6
M12-vim
Vimentin &
Ki-67
a
b
c
d
β-catenin
a′
b′
c′
d′
E-cadherin
a″
b″
c″
d″
C.
P69
M12
F6
M12-vim
α6-integrin
a
b
c
d
β4-integrin
a′
b′
c′
d′
α6-integrin
β4-integrin
a″
b″
c″
d″
D.
P69
M12
F6
M12-vim
α6-integrin
a
b
c
d
β1-integrin
a′
b′
c′
d′
α6-integrin
β1-integrin
a″
b″
c″
d″

Fig. 2

A.

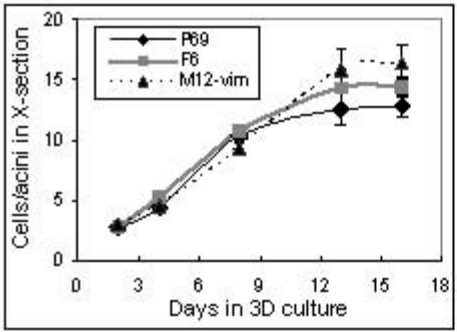
Cells/acini in X-section
20
15
10
5
0
0
3
6
9
12
15
18
Days in 3D culture
P69
F6
M12-vim

B.

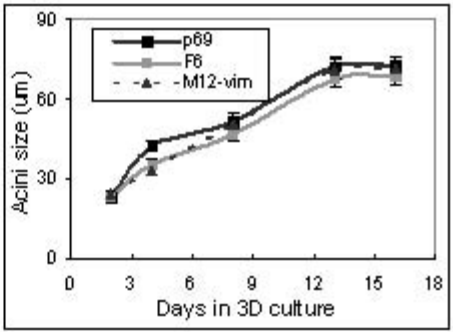
Acini size (um)
90
60
30
0
0
3
6
9
12
15
18
Days in 3D culture
p69
F6
M12-vim

Fig. 3

A.

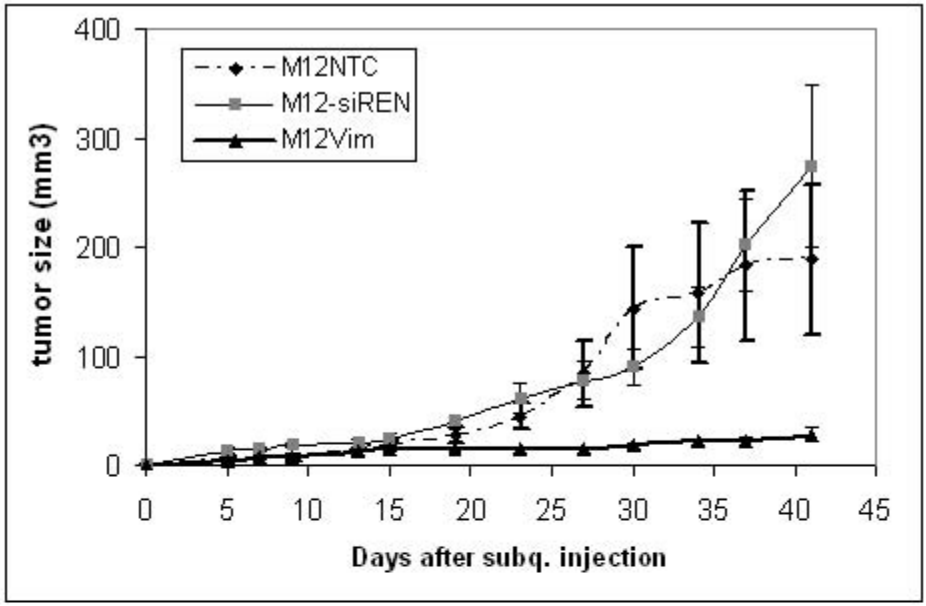
M12NTC
M12-siREN
M12Vim
tumor size (mm3)
400
300
200
100
0
0
5
10
15
20
25
30
35
40
45
Days after subq. injection

B.

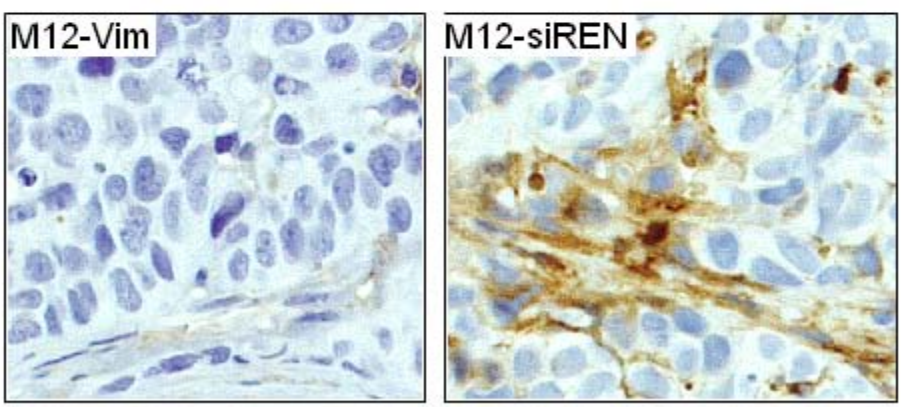
M12-Vim
M12-siREN

Fig. 4

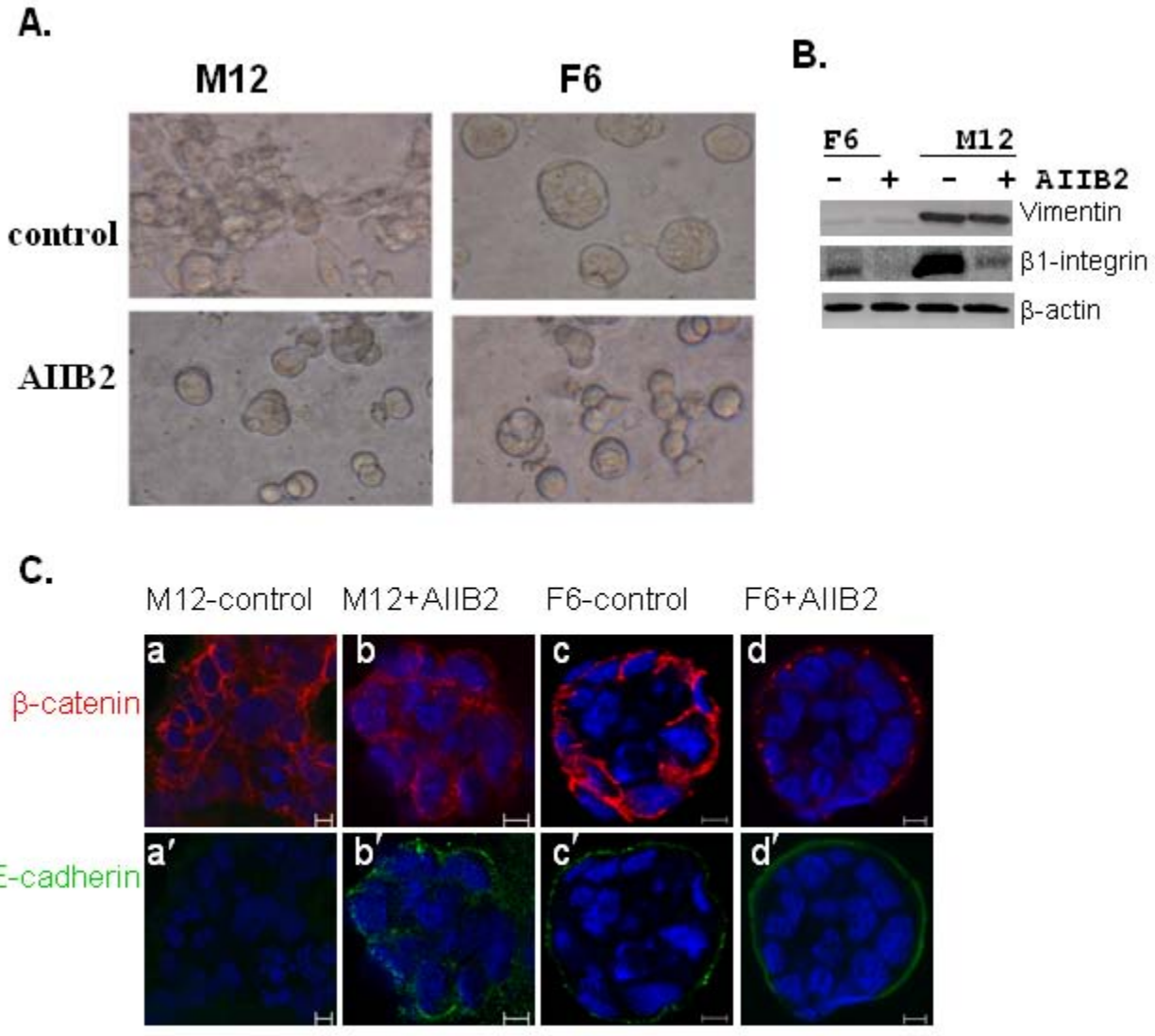
A.
M12
F6
control
AIIB2
B.
F6
M12
- + - + AIIB2
Vimentin
β1-integrin
β-actin
C.
M12-control
M12+AIIB2
F6-control
F6+AIIB2
β-catenin
E-cadherin
a
b
c
d
a′
b′
c′
d′

Fig. 5